

Tensile yielding of multiwall carbon nanotubes

Chenyu Wei^{a)}

NASA Ames Research Center, MS 229-1, Moffett Field, California 94035

Kyeongjae Cho

Department of Mechanical Engineering, Stanford University, California 94305

Deepak Srivastava

NASA Ames Research Center, MS 229-1, Moffett Field, California 94035

(Received 21 October 2002; accepted 15 February 2003)

The tensile yielding of multiwall carbon nanotubes (MWCNTs) has been studied using molecular-dynamics simulations and a transition state theory based model. We find a strong dependence of the yielding on the strain rate. A critical strain rate has been predicted above/below which yielding strain of a MWCNT is larger/smaller than that of the corresponding single-wall carbon nanotubes (CNTs). At an experimentally feasible strain rate of 1%/h and $T = 300$ K, the yield strain of a MWCNT is estimated to be about 3%–4% higher than that of an equivalent single-wall CNT. This is in good agreement with recent experimental observations. © 2003 American Institute of Physics. [DOI: 10.1063/1.1567041]

Carbon nanotubes (CNTs) have been the subject of extensive studies in recent years. In experiments, CNTs are grown in arc-discharge, chemical vapor deposition, and laser ablation based methods.¹ Single-wall CNTs (SWCNTs) and multiwall CNTs (MWCNTs) with many concentric shells of graphene type C layers are the common products depending on experimental conditions. Theoretical and experimental studies have shown that CNTs have exceptionally strong mechanical characteristics, with Young's modulus as high as 1 TPa. Many applications have been suggested to exploit the mechanical properties of CNTs and MWCNTs have been the main candidate as they can be produced in large quantities in experiments. The understanding of the mechanical response, such as yielding behavior, of MWCNTs is thus significantly important from the applications perspective.

Based on extensive molecular-dynamics (MD) simulations of yielding of SWCNTs, recently, we have proposed a transition state theory (TST) based model for the tensile failure of SWCNTs.² In the model, the tensile yielding strain is considered to depend on both the temperature and the strain rate. Starting with an Arrhenius description, the activation time for a yielding process is written as $t = (1/\nu) e^{E_v/k_B T}$, where E_v is the activation energy and ν is vibrational frequency. This can be expanded to $t = (1/\nu) e^{(E_v^0 - VK\epsilon)/k_B T}$ because E_v decreases linearly with applied tensile strain ϵ with K as the force constant and V as the activation volume. For the case of SWCNT, the tensile yielding is triggered by Stone–Wales (SW) bond rotation process, and E_v is the activation energy of formation of such defects (References on SW rotation and its static activation energy of formation are given in Ref. 3.) Detailed analysis shows that the yielding strain ϵ_Y can be obtained by inverting the above expression for the activation time as according to²

$$\epsilon_Y = \frac{\bar{E}_v}{VK} + \frac{k_B T}{VK} \ln \frac{N \dot{\epsilon}}{n_{\text{site}} \dot{\epsilon}_0}, \quad (1)$$

where \bar{E}_v is the averaged dynamic activation energy of SW bond rotations; $\dot{\epsilon}_0$ is the intrinsic strain rate; n_{site} is the number of atomic sites available for defect formation; and N is the number of SW bond rotations involved in the yielding process. The yield strain of a 60 Å long CNT(10,0) as a function of strain rate at different temperatures, shown in Fig. 1, was computed from extensive MD simulations (to be discussed next), and found to follow the relation expressed in Eq. (1). The intrinsic parameters obtained from the MD simulations data² for a CNT(10,0) are as following: $\bar{E}_v = 3.6$ eV; $\dot{\epsilon}_0/N = 8 \times 10^{-3} \text{ ps}^{-1}$; and $V = 2.88 \text{ Å}^3$ which is similar to that of the vacancy volume on a C atom on a CNT, and will be shown to play an important role in the yielding of MWCNT as well.

The dynamics and yielding of MWCNTs is the subject of interest in this letter. As a model, we consider a MWCNT made of two shells, CNT(20,0) (63.9 Å, 1200 atoms) and (10,0) (55.2 Å, 524 atoms). The capped inner shell is put concentrically and symmetrically inside the outer shell with

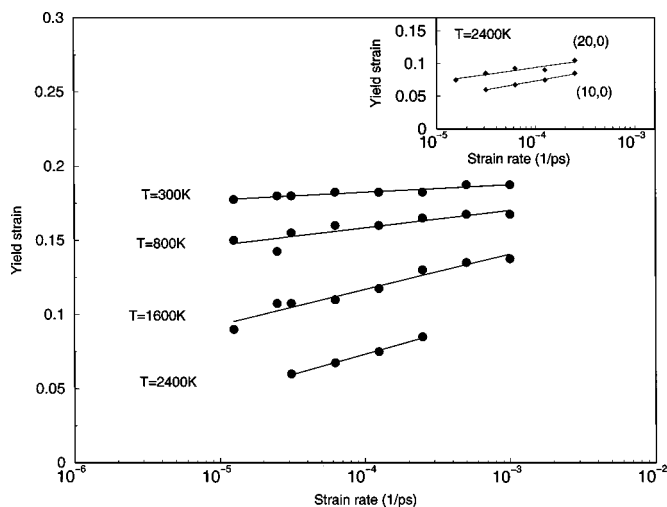


FIG. 1. The yield strain of a 60 Å long CNT(10,0) as a function of strain rate at various temperatures from 300 to 2400 K from MD simulations.

^{a)}Electronic mail: cwei@nas.nasa.gov

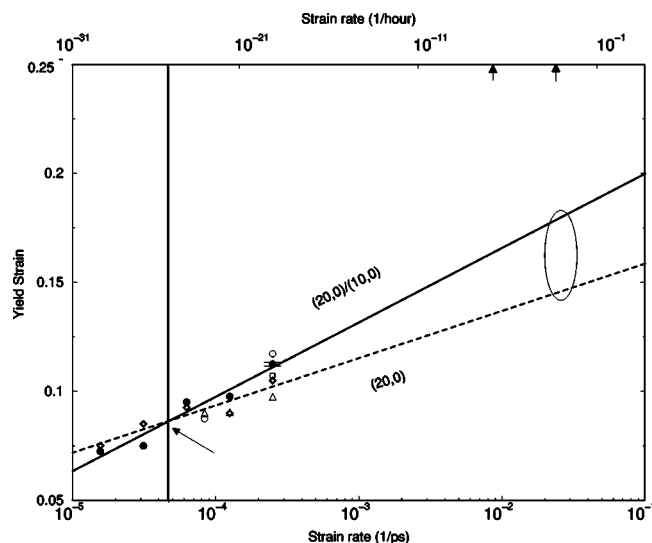


FIG. 2. The tensile yield strain of the (20,0)/(10,0) MWCNT (solid circle and line) as a function of strain rate at $T=2400$ K (bottom axis), in comparison to that of a CNT(20,0) (diamond and dashed line). The error bar at the point of strain rate of $2.5 \times 10^{-4} \text{ ps}^{-1}$ is calculated from data of five sample sets. The arrow in the lower left-hand side corner shows the cross-over point. The strain rate in the top axis corresponds to $T=300$ K, on which the marked positions show rates of 1%/h and 1%/year. The ellipse shows the range of experimental feasible conditions with strain rate as 1%/h at $T=300$ K. The data shown as open circle, open triangle, and open square are for (8,0)/(20,0), (12,0)/(20,0), and (5,5)/(10,10), respectively.

intershell spacing of 3.9 \AA . The tensile strain is gradually applied at the two ends of the outer shell (0.25% tensile strain per step followed by dynamics relaxation for a chosen time interval which is dependent on the strain rate). Any intershell load transfer is through van der Waals (VDW) interactions.⁴ Langevin friction force scheme⁵ is used to control temperature and time step is kept to 0.5 fs. The Tersoff–Brenner potential is used for C–C interactions, which can describe C bond formation and breaking. Details of this potential are described elsewhere.⁶

The MD simulations are conducted at a high temperature of 2400 K. Due to the tensile strain, the MWCNT (20,0)/(10,0) undergoes a yielding process initiated by the formation of SW bond rotation defects followed by the breaking of the outer shell, while the structure of the inner shell remains intact. The atomic structures are monitored and recorded during the dynamics. The yield strain is defined as the tensile strain at which the MWCNT behaves differently from its elastic behavior with an abrupt drop of the strain energy. The yield strain of MWCNT (20,0)/(10,0) as a function of strain rate, in comparison with that of a SWCNT (20,0) under similar conditions, is shown in Fig. 2. The standard error at a chosen point as shown in Fig. 2 is calculated from data of five sample sets. It is seen that the yielding of MWCNT has the similar logarithmic dependence on the strain rate as was observed for SWCNTs in our earlier work.² This is not surprising because we have assumed that the entire tensile strain is applied on the single outermost shell. The role of the inner shells in a MWCNT is to modify this behavior through VDW forces.

One important feature from Fig. 2 is that there is a critical crossover point $\dot{\epsilon}_{\text{cross}}$ of the strain rate $\dot{\epsilon}$ at which yield curves in the two cases cross. For $\dot{\epsilon}$ faster than $\dot{\epsilon}_{\text{cross}}$, the MWCNT has a larger yield strain compared with the equivalent SWCNT.

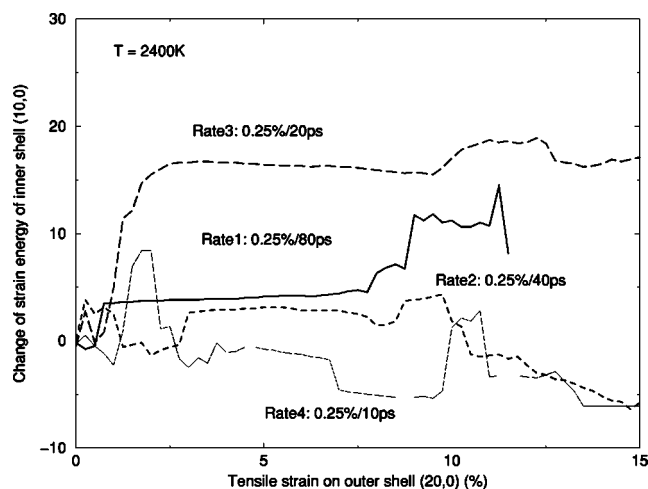


FIG. 3. The change of the strain energy of the inner shell CNT(10,0) as a function of the applied tensile strain on the outer shell CNT(20,0) at four strain rates at $T=2400$ K.

lent SWCNT. The situation is reversed for $\dot{\epsilon}$ slower than $\dot{\epsilon}_{\text{cross}}$. This feature can be explained by examining the intrinsic parameters that appear in Eq. (1). Experiments have suggested that for both dispersed SWCNT ropes and MWCNTs, Young's modulus is similar at 1 TPa.¹ The intrinsic strain rate and the number of processes involved in yielding are also expected to be of similar magnitude. A most probable parameter inducing the observed difference thus could be the activation volume. On one hand, smaller activation volume results in a larger yield strain at a fast strain rate, according to the intersection (first term) of the yield strain curve in Eq. (1). On the other hand, the yield strain decreases faster with a slow strain rate for the smaller activation volume. These two opposite effects result in a critical crossover point of the strain rate. By fitting the two curves in Fig. 2, we have (1) for a (20,0)/(10,0) MWCNT, $\epsilon_Y = 0.2339 + 0.0148 \ln \dot{\epsilon}$; and (2) for a (20,0) SWCNT, $\epsilon_Y = 0.1802 + 0.0094 \ln \dot{\epsilon}$. Assuming other parameters remaining same, the ratio of the activation volume on a MWCNT to that on a SWCNT is found to be $0.0094/0.0148 = 0.64$ or $0.1802/0.2339 = 0.77$ by comparing the slopes or the intersections, respectively. The two estimated values roughly agree with each other. The activation volume on the outermost shell of a MWCNT is thus found to be within 65% to 75% of that on an equivalent SWCNT shell.

A physical reason for the reduction of the activation volume on the outermost shell of a MWCNT can be explained as following. In the formation of SW bond rotation, a C—C bond rotates around its center by 90° to form a heptagon–pentagon pair. It has been shown that the out-of-plane rotation of the bond during the process provides a lower barrier pathway as compared to that of a totally in-plane rotation.⁷ The out-of-plane rotation of the C—C bond on the outer shell in a MWCNT is thus restricted to a smaller activation volume due to the VDW forces from the inner shells. Results of similar MD simulations on (8,0)/(20,0) and (12,0)/(20,0) MWCNT, with an intershell distance of 4.7 and 3.1 \AA respectively, are also shown in Fig. 2. The yield strain of the (12,0)/(20,0) MWCNT shows an enhanced activation volume effect (higher yield strain at fast strain rate and larger slope) due to smaller intershell distance, while the yield strain curve

for the (8,0)/(20,0) MWCNT is comparable with that of (20,0) CNT, suggesting that the larger intershell distance of 4.7 Å has a minor effect on activation volume. The yield strain of a (5,5)/(10,10) MWCNT, with intershell distance of 3.4 Å, at a strain rate $2.5 \times 10^{-4} \text{ ps}^{-1}$ is shown in Fig. 2. This shows that a MWCNT with armchair shells exhibit a similar increase as compared to MWCNTs with zigzag shells. Experiments⁸ have observed that MWCNTs with similar chirality shells are energetically favored over ones with changing chirality shells; thus, the later is unlikely to be made in experiments. Additionally, the changing chirality may add registry induced effects that may need separate investigations.

The critical crossover point in general cases can be estimated as follows. To have the same yield strain for systems with different activation volume, assuming other parameters remaining same, the following equation must hold for the strain rate at the crossover point $\dot{\epsilon}_{\text{cross}}$

$$\frac{\bar{E}_v}{K} + \frac{k_B T}{K} \ln \frac{N \dot{\epsilon}_{\text{cross}}}{n_{\text{site}} \dot{\epsilon}_0} = 0. \quad (2)$$

This means that

$$\dot{\epsilon}_{\text{cross}} = n_{\text{site}} \frac{\dot{\epsilon}_0}{N} e^{-\bar{E}_v/k_B T}, \quad (3)$$

where $\dot{\epsilon}_{\text{cross}}$ decays exponentially with temperature and is in the range of day^{-1} or smaller only for T above 1000 K. At $T=300 \text{ K}$, as shown in Fig. 2, $\dot{\epsilon}_{\text{cross}}$ is in the range of $10^{-25} \text{ year}^{-1}$. Thus, at room temperature, for all practical purposes, the yield strain of the outermost shell of a MWCNT is always considered to be larger than that of a SWCNT.

The aforementioned MD simulations were conducted at $T=2400 \text{ K}$. In usual experiments, the temperature is at 300 K, and strain rate is much slower, which is in the range of minute^{-1} or hour^{-1} . There is an equivalence between high temperatures with fast strain rates and low temperatures with slow strain rates. By rewriting Eq. (1), such an equivalence can be expressed as follows

$$\left(\frac{\dot{\epsilon}_1 N}{n_{\text{site}} \dot{\epsilon}_0} \right)^{T_1} = \left(\frac{\dot{\epsilon}_2 N}{n_{\text{site}} \dot{\epsilon}_0} \right)^{T_2}, \quad (4)$$

where Eq. (4) can be used to accelerate the yielding processes in the MD simulation by performing the simulations at high temperature and fast strain rates. In Fig. 2, the equivalent strain rate at $T=300 \text{ K}$, as according to Eq. (4) and with parameters listed in second paragraph with $n_{\text{site}}=1200$ for the MWCNT used in our simulation, is marked on the top axis. The range marked as an ellipse in Fig. 2 is for the strain rate of hour^{-1} at $T=300 \text{ K}$, which is usually used in experiments. It can be seen that in this range, the yield strain of the outermost shell of the MWCNT is about 3%–4% higher than that of the equivalent SWCNT shell. This is in qualitative agreement with recent experimental observations, where SWCNTs have been found to yield at up to 6% tensile strain^{9,10} and MWCNTs yield at 10%–12% tensile strain.¹¹

The change of the strain energy of the inner shell (10,0) is plotted as a function of the tensile strain on the outer shell (20,0) in Fig. 3 for four strain rate cases at $T=2400 \text{ K}$. For

small strains within 2%, all the cases show the sign of load transfers. For strains larger than that, the load transfer begins to cease, which suggests that the VDW forces between the shells is not strong enough to hold additional interfacial tensile stress. The strain energy curves fluctuate (possibly due to thermal fluctuations in the simulation) more for some strain rates than the others in this range and no clear trend is observed. With the tensile strain continuing to increase to a yield point, there is a sudden increase of load transfer (shown as the abrupt increase of strain energy at higher strains in Fig. 3), indicating the necking of the outer shell during the yielding process, which causes a pressure onto the the inner shell and helps more load transfers.

In summary, a recently proposed TST based model of tensile yielding of SWCNTs has been extended to explain the yielding of MWCNTs with the assumption that due to contact all the tensile strain is applied only to the outermost shell of the MWCNT. The yield strain of a two shell (20,0)/(10,0) MWCNT are computed through MD simulations and are found to decrease logarithmically with slower strain rate, in agreement with the underlying TST based model. A critical crossover strain rate is found below/above which yield strain of a MWCNT is smaller/larger than the equivalent SWCNT shell. This is attributed to the difference in the activation volume in the two cases, and the activation volume on the outermost shell of a MWCNT is found to be about 65% to 75% of that on an equivalent SWCNT. At room temperature, and experimentally feasible strain rates, the tensile yield strain of a MWCNT is found to be 3%–4% larger than the equivalent SWCNT which is in good agreement with recent experimental observations.

One of the authors (C.W.) is supported by NASA Contract No. AS-03 to Eloret Corp. and another author (D.S.) is supported by NASA Contract No. 704-40-32 to CSC, at the Ames Research Center.

¹For detailed review, see P. J. F. Harris, *Carbon Nanotubes and Related Structures: New Materials for the Twenty-first Century* (Cambridge University Press, Cambridge, UK, 1999).

²D. Srivastava, C. Wei, and K. Cho, *Rev. Appl. Mech.* **56**, 215 (2003); C. Wei, D. Srivastava, and K. Cho, *Phys. Rev. B* **67**, 115407 (2003).

³M. B. Nardelli, B. I. Yakobson, and J. Bernholc, *Phys. Rev. B* **57**, 4277 (1998); Q. Zhao, M. B. Nardelli, and J. Bernholc, *ibid.* **65**, 144105 (2002); G. G. Samsonidze, G. G. Samsonidze, and B. I. Yakobson, *Phys. Rev. Lett.* **88**, 65501 (2002).

⁴A 6–12 truncated Lennard-Jones-type potential is used with $\sigma=3.35 \text{ Å}$, $\epsilon=4.41 \text{ meV}$, and $r_{\text{cut}}=8.875 \text{ Å}$.

⁵J. C. Tully, Y. J. Chabal, K. Raghavachari, J. M. Bowman, and R. R. Lucchese, *Phys. Rev. B* **31**, 1184 (1985).

⁶J. Tersoff, *Phys. Rev. B* **37**, 6991 (1988); D. W. Brenner, *ibid.* **42**, 9458 (1990).

⁷P. Zhang, P. E. Lammert, and V. Crespi, *Phys. Rev. Lett.* **81**, 5346 (1998).

⁸A. Hassani, M. Tokumoto, S. Ohshima, Y. Kuriki, F. Ikazaki, K. Uchida, and M. Yumura, *Appl. Phys. Lett.* **75**, 2755 (1999).

⁹D. A. Walters, L. M. Ericson, M. J. Casavant, J. Liu, D. T. Colbert, K. A. Smith, and R. E. Smalley, *Appl. Phys. Lett.* **74**, 3803 (1999).

¹⁰M.-F. Yu, B. S. Files, S. Arepalli, and R. S. Ruoff, *Phys. Rev. Lett.* **84**, 5552 (2000).

¹¹M.-F. Yu, O. Lourie, M. J. Dyer, K. Moloni, T. F. Kelly, and R. S. Ruoff, *Science* **287**, 637 (2000).